Advances in Science and Technology Research Journal

Advances in Science and Technology Research Journal, 2026, 20(7), 557–571
https://doi.org/10.12913/22998624/220045
ISSN 2299-8624, License CC-BY 4.0

Received: 2026.03.02
Accepted: 2026.05.15
Published: 2026.06.01

Seismic response of steel geodesic domes with localized suspended mass

Dominika Bysiec[1], Tomasz Maleska[1*]

[1] Faculty of Civil Engineering and Architecture, Opole University of Technology, 45-758 Opole, Poland
* Corresponding author's e-mail: t.maleska@po.edu.pl

ABSTRACT

Lightweight steel geodesic domes are widely used in public structures and often support suspended equipment, which can affect their seismic performance. Understanding how such additional masses influence dynamic response is essential for safe design. In this paper, six steel geodesic dome models, shaped by two mesh topology methods, were numerically analyzed and subjected to three seismic excitations using DIANA FEA. Also, this paper evaluates displacements and accelerations for configurations without suspended mass, with mass at the dome center, and with mass offset by 10 meters. Results indicate that the dome topology significantly affects seismic response, and even small suspended masses (about 3.5–4.6% of the dome weight) can notably increase maximum displacements and accelerations, especially when centrally located. These findings suggest that both the structural topology and the placement of additional masses should be carefully considered in the seismic design of geodesic domes to ensure structural integrity under earthquake loading.

Keywords: geodesic domes, numerical analysis, seismic analysis, suspended mass, topology, lightweight structures.

INTRODUCTION

Dome roofs are primarily structures with large spans, which have many advantages. The popularization of steel construction makes them lightweight, which undoubtedly contributes to their increasingly widespread use (Figure 1). They are commonly used to cover public buildings, such as stadiums, exhibition halls, shopping centers, airport terminals, and sports fields. Therefore, they require meticulous research into their durability to ensure the safety of many people who stay in them (Schling et al., 2022). In recent years, many papers have analyzed various aspects of this type of roofing. Detailed analyses of dome stability, cross-section optimization, topology, geometry, and dynamic response were included. All these make dome-shaped structures increasingly used by architects and constructors.

Dome optimization has received particular attention, especially as many papers have recognized this aspect. The use of various optimization algorithms aims to obtain lighter structures that require less construction material by optimizing the cross-sections of their individual elements. Grzywiński et al. (2019) used the Jaya meta-heuristic algorithm. Kaveh and Talatahari (2011) used a charged system search algorithm to optimize the geometry and topology of the domes under consideration. Gholizadeh and Hamed (2014) presented the firefly algorithm (FA) and particle swarm optimization (PSO) for optimizing the topology of nonlinear single-layer domes. Another optimization approach was proposed by Pilarska (2020, 2021), Bysiec (2023), and Bysiec et al. (2024), pointing to the use of an appropriate method of shaping the topology of the geodesic dome mesh, which is consequently reflected in the lower weight of the covering and less construction material. In these papers, weight reductions of up to 17% were achieved, which turned out to be more beneficial than the use of improved algorithms.

Each structure, including a domed covering, requires monitoring of its technical condition, a process aimed at preventing its destruction. Any

Figure 1. Example of lightweight structures: a) geodesic dome in a residential house in Milan (Italy), b) roof of a shopping mall in Warsaw (Poland)

structural damage, as well as changes in static or dynamic loads, can affect the structure's behavior and, consequently, lead to its destruction. In the case of large, complex structures, identifying damage is difficult. A relatively small number of measurements and identified local damages have a limited impact on the entire structure. The change in static loads, resulting from the suspension of additional mass, may significantly affect the research and analysis carried out to monitor the technical condition of the structure in a global aspect, i.e., the safety and use of the entire structure.

Increasing loads by introducing additional mass into the structure may be indicated by a layer of snow or ice on the roof covering or by additional devices or equipment suspended to the structure. In the paper Fanning and Carden (2004), a mass of additional devices mounted on telecommunications masts was analyzed, without the need to dismantle them. Using a genetic algorithm, Ostachowicz et al. (2002) examined the identification of the position of a mass concentrated on an isotropic plate. Moreover, the possibility of using this technique to identify the exact location of the concentrated mass and determine its value was indicated. A similar problem was considered by Piatkowski and Waszczyszyn (2011). The authors used Recurrent Cascade Neural Network techniques in this case for a steel plate. Nalitolela et al. (1993) added stiffness to the original structure, thereby constructing a new structure with new frequency response functions based on the original structural response information. Liquid, as a factor affecting the structure's mass, was used to identify damage on a submerged cantilever beam and a liquid storage tank (Dems and Mroz, 2010). To obtain a change in the dynamic characteristics, Rajendran and Srinivasan (2016) attached a mass to different places of the composite plates.

Many construction failures or disasters are associated with a layer of snow or ice on the structure. These factors often result in a significant increase in loads, especially on roof structures. The 2006 disaster at the Katowice Fair Building in Poland shows that additional snow load is one of several causes of its collapse. The fundamental construction error was the low strength of individual structural elements of buildings (Biegus and Rykaluk, 2009). Similarly, residual snow was one of the factors contributing to the collapse of a spatial truss covering a reinforced concrete structure in Turkey in 2003 (Caglayan and Yuksel, 2008). In this paper, the authors point to the underestimation of the snow load intensity and errors made in the truss construction.

Domed roof coverings are also susceptible to disasters due to the load imposed by snow. An example of the effects of local structural overload is the disaster of two spherical pavilion covers in Chorzów, Poland, in the winter of 1967/68. The displacement of the accumulated snow from the

windward to the leeward side of the dome's covering, under the influence of strong winds, led to its collapse (Augustyn and Śledziewski, 1976). A layer of snow and ice, along with construction errors, destroyed a 500 m^2 steel, concrete, and glass dome covering the Transvaal Aquapark building in Eastern Europe in 2004 (Lapin et al., 2019). In turn, in 2006, similar reasons led to the disaster of the Basmanna market dome, also in that region.

However, the analysis of lightweight structures subjected to seismic excitations has rarely been undertaken in the literature. Papers on the behavior of geodesic dome structures under seismic loads were presented by Bysiec and Maleska (2021, 2023), indicating the need to select an different method for shaping their topology. However, conducting a detailed dynamic analysis of the domes enables a thorough understanding of the structure's behavior and monitoring the progression of a possible progressive disaster. Such a study was conducted by Tian et al. (2021) on a simplified long-span single-layer spatial grid structure model. They showed that progressive structural collapse can be mitigated when dynamic interactions are considered. In turn, Zhang et al. (2022) presented a procedure for calculating the element importance factor to evaluate the stiffness of critical elements of a mesh dome structure. They used a global stiffness matrix for the Kiewitt, Schwedler, and other reticulated domes.

In the case of dynamic loads such as earthquakes, the concept of additional mass is completely different because, in most cases, it is a structural element of a given building. There are papers in the literature that use additional mass as a vibration damper, allowing the object to survive a strong earthquake. This was particularly important for tall, strategic buildings, such as skyscrapers, power plants, and bridges (Shu et al., 2017; Zhang et al., 2023; Acito et al., 2021). Then, introducing additional mass was desirable to ensure the structure's and its users' safety.

Therefore, as mentioned earlier, additional mass may be desirable, and thanks to it, the structure will ensure safe transfer of external loads. However, there are cases where the additional mass on the supporting structure caused a disaster and the deaths of people. In the case of lightweight structures, it is necessary to analyze whether suspending a small amount of additional mass, i.e., devices constituting the facility's equipment, cooling devices, sound systems, or telescreens, will affect the behavior of the structure as a result of a given dynamic load (e.g., earthquake). Based on a literature review, it is difficult to define clearly because these are relatively light masses. In turn, it should be noted that very light structures are usually made of steel or aluminium, and their designed load capacity utilization for a given load is almost 100%. It is appropriate to seek an answer to this troubling question. Moreover, whether the mass location is important, especially under dynamic loads. According to the authors of this paper, it is possible because it may disrupt the ideal structure (e.g., geodesic dome) and its design assumptions.

Therefore, this paper aims to investigate the effect of additional mass suspended to the structure (a type of utility equipment or device) of low weight relative to the entire structure of a steel geodesic dome subjected to earthquakes. The DIANA FEA numerical program was used to determine the impact. However, three seismic excitations with different intensities and durations of the seismic record were used to obtain a dynamic response. The paper analyzed displacements and accelerations, i.e., the values required to be determined in various standards (ASCE 7 2022, Eurocode 8 2005).

DESCRIPTION OF GEODESIC DOMES

General remarks

The geodesic domes used in this paper as the basis for the analysis were shaped using two methods. Different connections of the edge division points of the initial regular octahedron allowed the creation of different topologies of meshes of the analyzed structures.

Extended procedures for forming geodesic domes derived from a regular octahedron, using two different methods, can be found in the papers by Pilarska (2020, Bysiec (2023), and Bysiec et al (2024). Moreover, the papers (Bysiec nad Maleska 2021; Bysiec et al. 2023) show that the method of shaping the topology of these covers has a significant impact on the consumption of the construction material (steel) and the behavior of the structure under a given load.

In this paper, two developed geodesic domes subjected to seismic excitations were shaped using two methods proposed by Fuliński (1978). The structures were designed based on regular octahedra, subdividing their equilateral faces

into smaller subfaces and using the resulting face vertices to define the nodes of the structural grid. Meanwhile, the edges of the subfaces define the axes of the structural steel members. The two methods analyzed led to the division of the initial triangle of the octahedron into smaller triangles, with frequency (V) indicating the number of subdivisions. This subdivision process automatically generates a three-way grid on every face of the basis octahedron. The major view of this grid's vertices on the octahedron's circumscribed sphere leads to a polyhedron approximating the sphere in which only the grid's nodes lie on the sphere's surface. Other, higher frequencies give smoother spheres. These methods were described in detail in Pilarska's (2020) paper. Figure 2 shows the difference in the shaping of geodesic domes using the first and second subdivision methods.

Figure 3 shows two models of geodesic domes used to conduct this analysis, generated based on two methods (Figure 4) of connecting their elements: (i) 2888-hedron strut dome (method 1 – model I^1 – Figure 5a) and (ii) 2904-hedron strut dome (method 2 – model I^2 – Figure 5d).

The influence of additional mass suspended in two different places on the structure was considered, thanks to which another four models were obtained, i.e., additional mass located in the middle of the dome span (model II^1 – Figure 5b and model II^2 – Figure 5e) and suspended at a distance of approximately 10 meters from the central point (model III^1 – Figure 5c and model III^2 – Figure 5f). The placement of the additional mass was based on the authors' previous research (Bysiec et al., 2023) and the practical application of the suspended additional mass in the dome.

The suspended mass weighed 2 tons and was attached to the structure node. Ultimately, six models were tested and presented in Figure 3. The additional mass used is a type of equipment: devices mounted to the roofs of lightweight structures. Placing it at the center of the dome will maintain the structure's perfect symmetry. However, finding the additional mass at a certain distance from the central point, for example, 10 meters from the top of the dome, will undoubtedly affect the entire structure layout, as shown in models III^1 (Figure 5c) and III^2 (Figure 5f). In addition, the additional mass was fixed to the steel structure.

Material properties

In this research, the geodesic domes are covers made of steel struts (round pipes) of S235 standard steel. The steel elements were modelled as linearly elastic, isotropic materials, according to Eurocode 3 (2005) and Bysiec and Maleska (2021), with the properties tabulated in Table 1.

In this type of structures, round pipes are most often used, which, thanks to their advantages of stiffness in all directions, allow for the safe transfer of external loads. Therefore, in this paper (as in the papers by Pilarska (2020) and Bysiec and Maleska (2021)), the steel strut elements of domes were divided into four groups (Table 2). Depending on the method used to shape the dome structure, the strut diameters varied, and therefore, the dome weights differed. For the dome shaped according to method 1, its weight was 57.9 tons, and for method 2, it was 43.6 tons.

Seismic excitation

Three seismic records were used to estimate the most accurate response of the steel dome structures to seismic excitation: (i) Ancona from

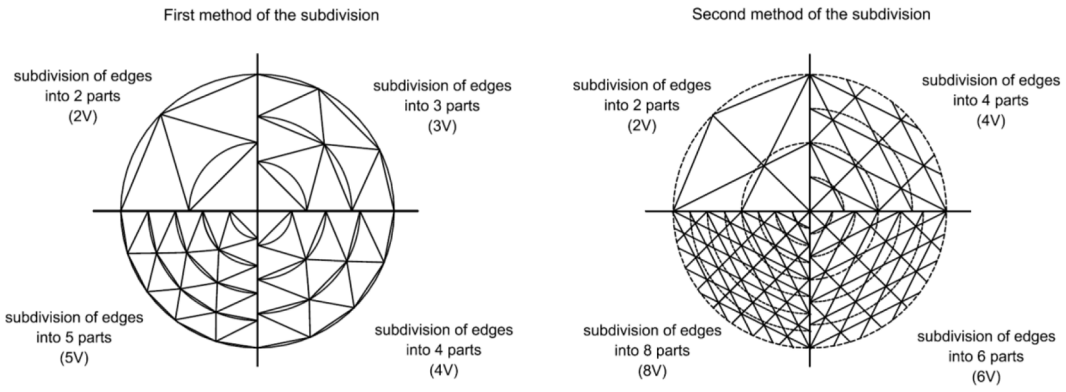

Figure 2. Methods of subdividing the initial triangle edge, based on Fuliński

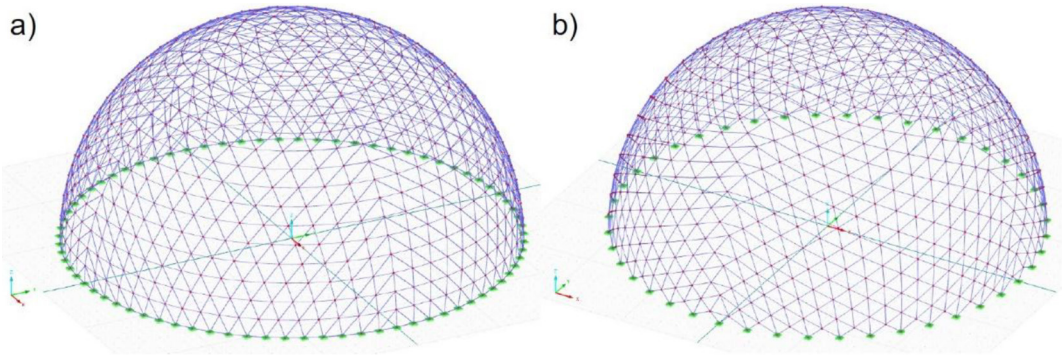

Figure 3. Structures used in conducted analysis: a) 2888-hedron strut dome (method 1 – model I^1 – III^1), b) 2904-hedron strut dome (method 2 – model I^2 – III^2

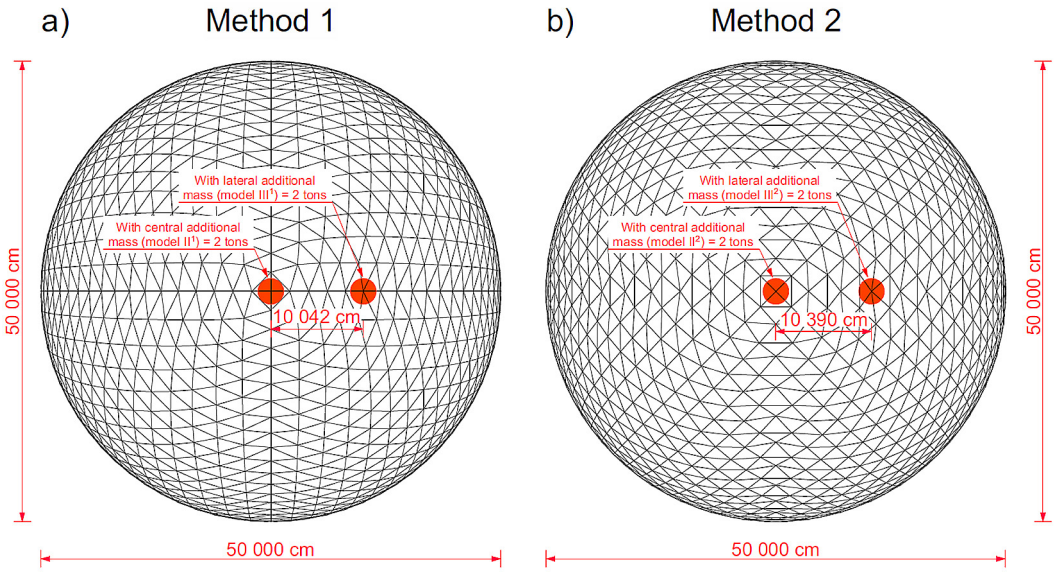

Figure 4. View of the geodesic domes with additional mass for method: a) 1 (2888-hedron strut dome), b) 2 (2904-hedron strut dome)

1972 (Figure 6a), (ii) Denizli from 1976 (Figure 6b), and El Centro from 1941 (Figure 6c).

These three seismic records differ in the duration and length of the earthquake's intensity zone. Obviously, the El Centro record was characterized by a magnitude of 6.9 on the Richter scale, which was the so-called Benchmark for seismic analysis of building structures. The remaining records (Ancona and Denizli) were slightly weaker but had a similar maximum ground acceleration to the El Centro record. The El Centro record owes its destructive power to its relatively high intensity compared to the other records examined (Ancona and Denizli). The three records examined are required by Eurocode 8 (2005) to determine the structure's behavior under seismic excitations. That is why this number of seismic records was adopted in this numerical analysis. The aim of the paper was also to show how important the earthquake duration and the length of the intense zone were. Some standards omit this important aspect, CHBDC (2017), which, according to the authors, is a wrong approach. In this numerical study, seismic excitation was applied simultaneously to the base of the geodesic dome models in three directions: X – horizontal, Y – horizontal, and Z – vertical.

Validation of the numerical model

The numerical model was validated based on the assumptions of structural mechanics, recommendations for modeling in DIANA FEA, and the authors' previous experience with this research. An experiment on a real scale is impossible because the tested domes have a diameter of about 50 meters.

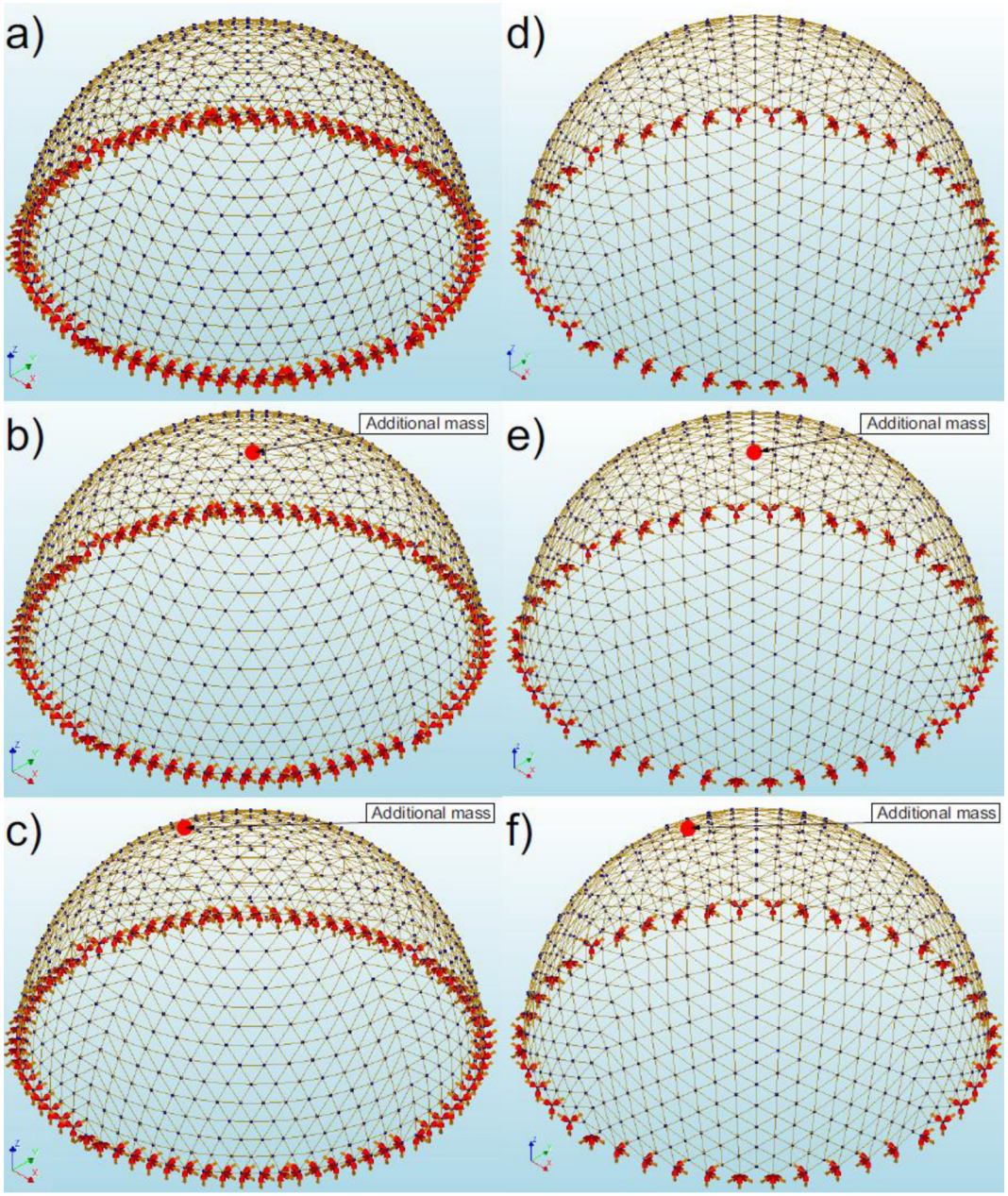

Figure 5. Models of geodesic domes from DIANA FEA: a) I^1, b) II^1, c) III^1, d) I^2, e) II^2, f) III^2

In turn, constructing a scale model is impossible because these structures are made of thin-walled pipes, which have a relatively large moment of inertia given their low weight. Constructing the dome on a scale would, therefore, undoubtedly disrupt this feature of lightweight structures.

RESULTS OF NUMERICAL ANALYSIS

General remarks

Using the numerical program DIANA FEA, the impact of seismic excitations on the analyzed six models of geodetic dome structures was determined. The program used is based on the finite element method. A nonlinear analysis of the behavior of dome structures under the influence of Ancona, Denizli, and El Centro seismic excitations was carried out. The behavior of the domes over time was examined using the Time History method, a commonly used method for determining the response of various structures to seismic excitations (Maleska and Beben 2023a,b). The Time History method is based on analyzing the structure at the particular time steps specified in the numerical model. This means that the whole structure was analyzed for the seismic response at

Table 1. Properties of steel struts

Steel properties according to Eurocode 3 (2005)	Value
Young's modulus (*E*)	210 GPa
Kirchhoff's modulus (*G*)	80.76 GPa
Poisson's ratio (*ν*)	0.3
Thermal expansion coefficient (*α*)	1.2×10^{-5}
Volumetric weight (*γ*)	7850 kg/m^3

Table 2. Steel groups of struts for geodesic dome

Group of struts	
model I^1, II^1, III^1	model I^2, II^2, III^2
RO 70.0 x 8.0	RO 70.0 x 7.1
RO 63.5 x 8.8	RO 63.5 x 8.0
RO 44.5 x 5.6	RO 57.0 x 5.6

individual time steps (0.02 s) throughout the seismic excitations (Figure 6). It should be emphasized that this method is based on the modes of natural vibrations. In the tested models, 20 modes of natural vibration were determined, intended to account for theoretical frequencies that cannot be measured in the structure's real operating conditions. This research paper concentrates on the typical values of seismic analysis, i.e., displacement and acceleration (Tables 3 and 4). The tests were carried out for three variants (Figures 4 and 5): (i) without a suspended mass, (ii) with a suspended mass in the central point of the dome, (iii) with a suspended mass located about 10 m from the central point of the dome, for domes created according to two different methods of the mesh topology shaping, using three different seismic excitations (Ancona, Denizli, El Centro – Figure 6). Taking the above into account, 18 numerical models were finally analyzed. It should be added that in models I^1 (Figure 5a) and I^2 (Figure 5d) no additional mass was suspended, in models II^1 (Figure 5b) and II^2 (Figure 5e) the mass (2 tons) was suspended in the middle (Figure 4a) of the dome span, and in models III^1 (Figure 5c) and III^2 (Figure 5f) the mass (2 tons) was displaced from the center by about 10 m (Figure 4b).

Displacements

Based on the numerical tests (Table 3), the highest values were obtained for model II^1 (Figure 7b), in which the dome was shaped according to method 1. It can be seen that using individual methods to shape the strut mesh in a geodesic dome affects the resulting values. First of all, it can be noticed that the results from models I^1, II^1, and III^1 were much higher for the more destructive records, i.e., Denizli and El Centro.

In these models, it can also be seen how important recording intensity and duration are (Denizli: about 16 seconds; El Centro: about 56 seconds). Interestingly, in models II and III for the Denizli and El Centro records, higher displacement values were obtained for method 1 than in models II^2 (Figure 7e) and III^2 (Figure 7f), which were shaped according to method 2.

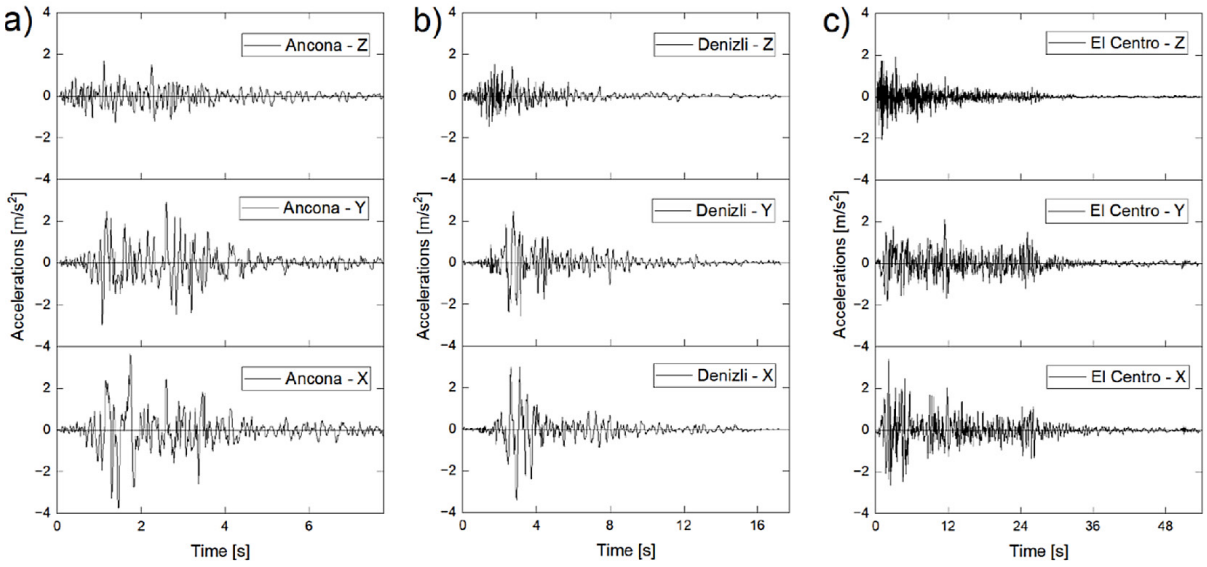

Figure 6. Seismic record on particular direction from numerical analysis: a) Ancona, b) Denizli, and c) El Centro

Table 3. Results of maximal displacements from numerical analysis

Type of mass	Method	direction	Ancona [mm]	Denizli [mm]	El Centro [mm]
Without additional mass (model I)	1(2888-hedron)	X (TrDtX)	7.52	21.83	-88.39
		Y (TrDtY)	7.70	-15.13	60.45
		Z (TrDtZ)	8.25	-13.89	-42.68
	2(2904-hedron)	X (TrDtX)	9.07	-17.48	-65.78
		Y (TrDtY)	-7.24	18.95	89.98
		Z (TrDtZ)	-10.65	23.81	75.98
With central mass (model II)	1(2888-hedron)	X (TrDtX)	8.17	22.52	-124.78
		Y (TrDtY)	7.58	13.04	108.43
		Z (TrDtZ)	-6.76	-13.12	-61.28
	2(2904-hedron)	X (TrDtX)	9.07	-17.28	-69.36
		Y (TrDtY)	7.32	-18.49	86.40
		Z (TrDtZ)	-12.62	23.41	61.17
With distance mass (model III)	1(2888-hedron)	X (TrDtX)	7.56	27.02	-119.49
		Y (TrDtY)	7.78	-13.32	105.92
		Z (TrDtZ)	8.09	-13.37	-64.24
	2(2904-hedron)	X (TrDtX)	8.99	-16.69	-73.27
		Y (TrDtY)	7.17	-18.09	84.71
		Z (TrDtZ)	-10.65	24.86	80.03

Table 4. Results of maximal accelerations from numerical analysis

Type of mass	Method	direction	Ancona [m/s^2]	Denizli [m/s^2]	El Centro [m/s^2]
Without additional mass (model I)	1(2888-hedron)	X (TAtX)	4.06	3.65	19.12
		Y (TAtY)	3.75	3.41	14.65
		Z (TAtZ)	4.89	4.86	14.99
	2(2904-hedron)	X (TAtX)	1.45	1.69	4.34
		Y (TAtY)	1.32	1.66	4.01
		Z (TAtZ)	2.08	2.23	5.28
With central mass (model II)	1(2888-hedron)	X (TAtX)	3.72	4.12	25.72
		Y (TAtY)	3.79	3.74	35.59
		Z (TAtZ)	4.84	5.52	29.88
	2(2904-hedron)	X (TAtX)	1.39	1.65	5.09
		Y (TAtY)	1.32	1.69	4.14
		Z (TAtZ)	2.06	2.22	4.79
With distance mass (model III)	1(2888-hedron)	X (TAtX)	3.57	4.38	31.58
		Y (TAtY)	3.56	3.89	31.88
		Z (TAtZ)	4.88	5.36	32.11
	2(2904-hedron)	X (TAtX)	1.44	1.63	5.00
		Y (TAtY)	1.34	1.62	4.35
		Z (TAtZ)	2.05	2.29	4.46

In turn, for models I, II, and III for the Ancona record, a completely different tendency is observed than for the Denizli and El Centro records, i.e., higher displacement values for method 2 of shaping the strut mesh.

This shows that the effect of recording length was significant, as illustrated in Figure 8. An increase in the value of displacements with increasing recording duration was evident. Therefore, it is not the maximum recorded acceleration

that determines the impact on geodesic dome structures, but the recording duration. However, it was visible that adding additional mass was also important. Interestingly, this had a greater impact in the case of model II than model III.

Considering the places where the maximum displacement values occurred, it can be concluded that method 1 (Figure 7a,b,c) was more predictable because the maximum values appeared around half the height of the structures. In method 2, the situation was more complex because there was no clear trend as in method 1. In method 2, the maximum values appeared very randomly, e.g., Figure 7d shows that the maximum displacements were recorded near the lower rings of the dome.

In turn, Figure 7e shows that the maximum values occurred near the center of the dome (where the additional mass was suspended). In Figure 7f, it can be seen that the place of maximum values was around the mid-span, as was the case in method 1 (Figure 7a,b,c).

It is worth emphasizing that suspending additional mass to the structure can affect displacements (Table 2, Figure 7, 9), especially given the additional mass's low relative weight to the entire structure. The suspended mass was 2 tons, which was 3.5% (method 1) and 4.6% (method 2) of the total weight of the domes considered. The impact on displacement values was especially evident in El Centro, where increases of 41% were observed between individual models. However, it can be observed that with a robust El Centro record, the effect of additional mass in method 2 was even beneficial, as a reduction in model III compared to model I of about 6% was observed.

As the analysis showed, the location of the additional mass in the dome structure was also important, which may seem obvious. This phenomenon was observed only in models that used a very strong earthquake, such as the El Centro earthquake. In model III (Figure 9i), displacements were reduced compared to model II (Figure 9f), where the mass was located centrally at the top of the dome. Moreover, adding additional mass in the structure (models II and III) resulted in greater disruption of the relatively uniform seismic response of the domes (method 1 – Figure 9c, f, i).

Accelerations

Based on the results presented in Table 4 and Figure 10, the highest accelerations were recorded for the El Centro record, i.e., the longest and highest-strength record. The highest acceleration value was recorded in model II[1] (Figure 10b) in the horizontal direction (Y) for the analyzed models. This value was consistent with the maximum displacements appearing in the same model (Figure 7b). In the other analyzed cases, it was observed that the acceleration values increased with the earthquake's strength and duration. Therefore, the smallest ones occurred in the Ancona record. Moreover, it should be noted

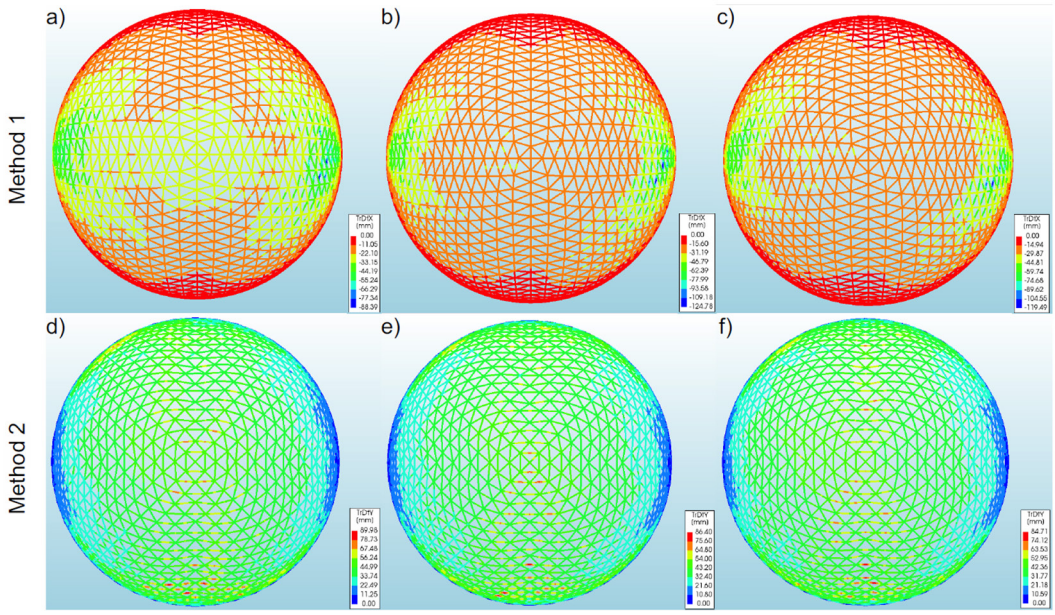

Figure 7. Maximum displacements from El Centro record for models: a) I[1], b) II[1], c) III[1], d) I[2], e) II[2], and f) III[2]

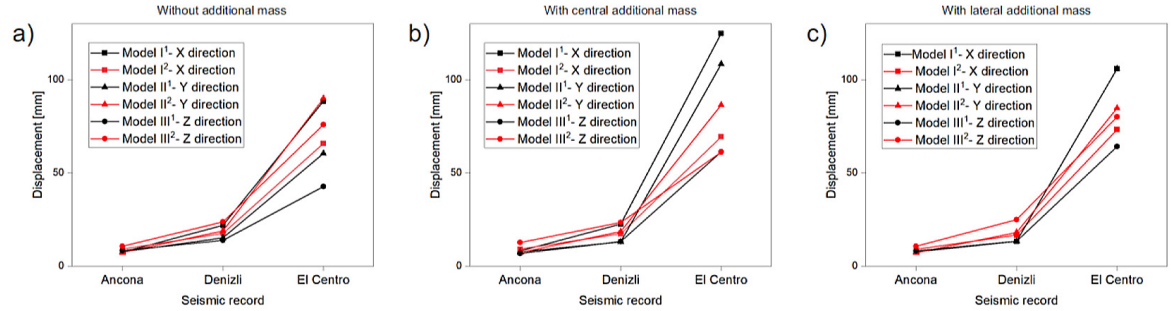

Figure 8. Tendency in numerical analysis based on displacements for models: a) without additional mass – model I, b) with central additional mass – model II c) with lateral additional mass – model III

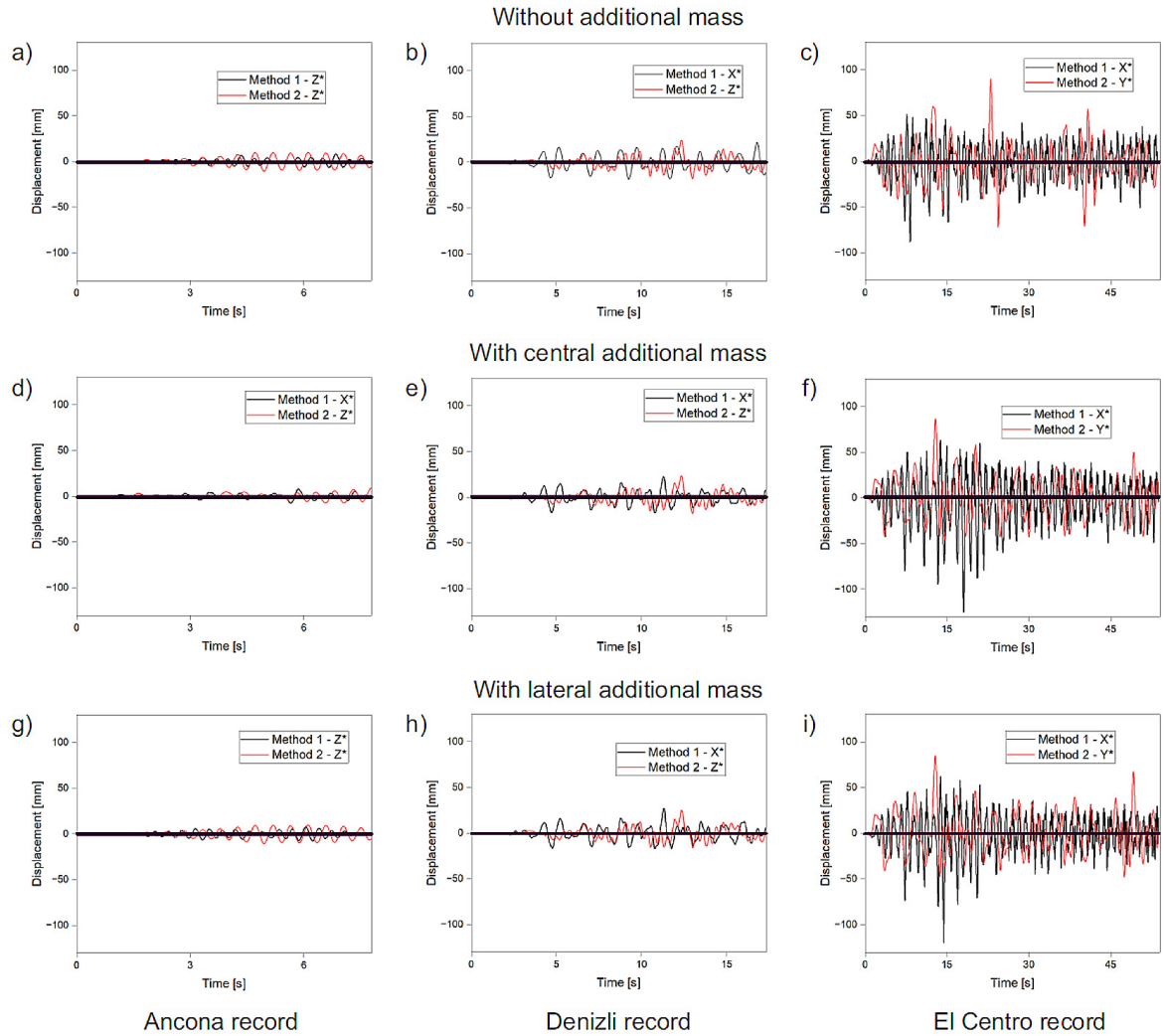

Figure 9. Maximum displacements in time for models: I (a) Ancona, b) Denizli, and c) El Centro record), II (d) Ancona, e) Denizli, and f) El Centro record), III (g) Ancona, h) Denizli, and i) El Centro record)

that the highest values were recorded for method 1 of shaping the geodesic dome structure.

The locations of the maximum accelerations were very similar to those of the displacements. In method 1, the maximum accelerations were recorded around half the height of the numerical model of the dome (Figure 10a,b,c), which results from the maximum displacements. However, in method 2 for shaping the dome strut mesh, the locations of the maximum accelerations were

more random. In the I^2 (Figure 10d) model, the maximum values were recorded in the lower parts of the dome. However, for models II^2 (Figure 10e) and III^2 (Figure 10f), these were around the center of the top of the dome and half the height of the dome, respectively.

In the case of mounting additional mass in the structure, the question arises (as with displacements) whether it affects the maximum acceleration values, despite the small weight of the additional mass (2 tons). It can be seen that this impact was significant for method 1, where the acceleration values in model II^1 increased by up to 86% compared to model I^1. In turn, in method 2, this impact was noticeable but less pronounced than in method 1

Attention should also be paid to the influence of mass location in the dome structure. In method 2, model III^2 (El Centro record – Figure 10f) achieved a reduction of even 6% compared to model II^2 (Figure 10e). If we look at the weaker records, i.e., Ancona and Denizli, the difference was subtle and reached only about 3%.

Moreover, attention should be paid to the fact that, in the case of weaker records (Ancona - Figure 11a,d,g and Denizli - Figure 11b,e), the maximum acceleration values reach their peak and then return to the starting point. In the case of the Ancona record, it does not matter which model was analyzed, since the record was short. Denizli's record caused a more significant problem for the steel structure of the dome, particularly for the dome created using method 1 to form the sphere of this structure. Moreover, based on Figure 12, it can be concluded that the impact of seismic excitations on method 1 was more pronounced for accelerations than for displacements (Figure 8). The advantage of method 2 over method 1 was especially evident when we added additional mass to the dome structure (model II – Figure 12b and model III – Figure 12c).

DISCUSSION

As described in the introduction, the impact of different mass locations in geodesic dome structures under highly random loads, such as seismic excitations, has not been analyzed so far. The papers by Bysiec and Maleska (2021, 2023) examined the impact of shocks on the domes but did not consider the additional mass suspended to the structure. Compared to the papers by Bysiec and Maleska (2021, 2023), this research raises another important aspect: in addition to recording intensity, the additional equipment (sound system, lighting, devices, etc.) of the steel structure of the dome is also important. In the indicated papers, the authors showed that the maximum accelerations and displacements usually occurred in horizontal directions in most cases studied. However, as shown in this paper, the use of additional mass (the suspended mass was 2 tons, which was 3.5% (method 1) and 4.6% (method

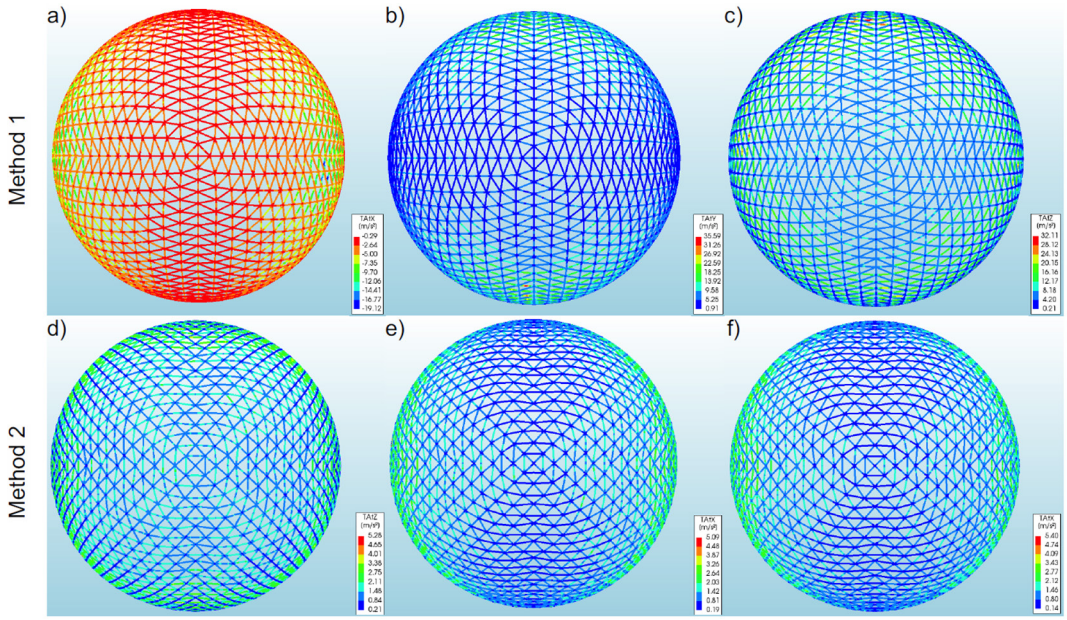

Figure 10. Maximum accelerations from El Centro record for model: a) I^1, b) II^1, c) III^1, d) I^2, e) II^2, and f) III^2

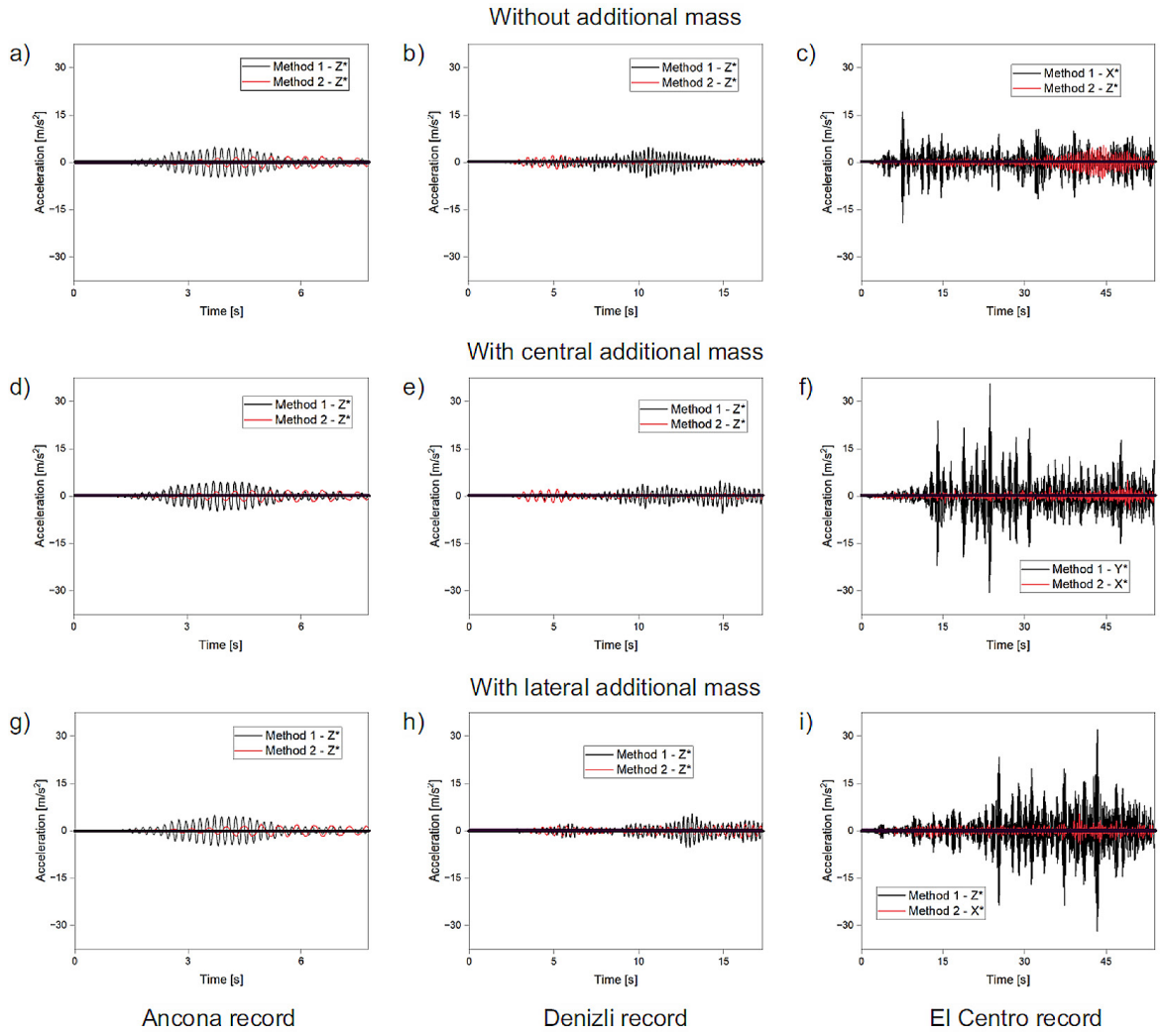

Figure 11. Maximum accelerations in time for model: I (a) Ancona, b) Denizli, and c) El Centro record), II (d) Ancona, e) Denizli, and f) El Centro record), III (g) Ancona, h) Denizli, and i) El Centro record)

2) of the total weight of the domes considered) resulted in maximum values of displacements and accelerations appearing also in the vertical direction in some cases.

In turn, the papers (Takeuchi et al. 2007; Nakazawa et al. 2012; Li and Xu 2014) did not thoroughly examine the dynamic characteristics of geodesic domes. The Authors examined only the displacement or acceleration, which, according to the authors, does not properly present the problem of the response of lightweight structures to seismic excitations.

Nair et al. (2021) investigated the effects of higher substructure modes on the roof response and developed amplification factors for dome grid shell roofs with multistorey substructures. However, the influence of recording length was not analyzed, which, as shown in this paper and the papers by Bysiec and Maleska (2021, 2023), significantly affects the behavior of the steel geodesic dome structure. Therefore, the dynamic response of the entire steel dome structure changes.

In the paper (Fan et al., 2022), the acceleration response of single-layer spherical reticulated shell nodes under earthquake action was compared with that of non-structural components in current seismic design codes, and the elastic acceleration response spectra of single-layer spherical reticulated shell nodes under earthquakes were studied. In addition, numerical analysis of lightweight structures is difficult due to their large size. Undoubtedly, the results of this paper helped to approach the problem appropriately and solve it in the best possible way, which, according to the paper's authors, was presented in the text.

Based on the discussion of the results, one of the limitations of the conducted research is the fact that it was conducted for domes with large

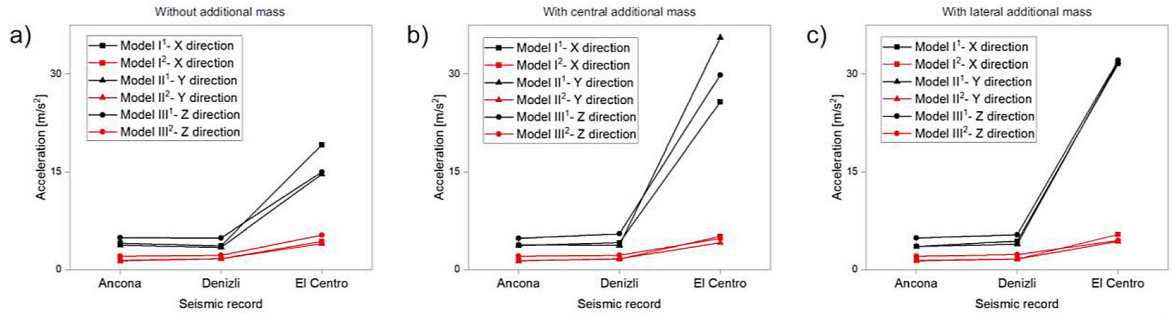

Figure 12. Tendency in numerical analysis based on accelerations for models: a) without additional mass – model I, b) with central additional mass – model II c) with lateral additional mass – model III

spans (50 m). Therefore, analyzing these research results for smaller domes may be problematic, as geodesic domes leverage steel's greatest advantage: the ability to transfer large tensile forces with minimal steel consumption. As a result, the impact of additional masses with similar weights (2 tons) as in this paper may give completely different results and villages.

CONCLUSIONS

Based on the analysis, it can be seen that different methods for shaping the steel geodesic sphere affect its dynamic response under a given seismic load. Additionally, it can be observed that suspending a small mass from the structure also affects the maximum values of displacement and acceleration.

Moreover, it is worth noting that:

- Method 2 of shaping the dome's mesh suppresses the impact of a seismic shock better than method 1. This is because both domes were constructed using different dome shaping methods, as detailed in Pilarska (2020). The impact of each method (method 1 or 2) also translates into different steel consumption,
- The dome with a smaller weight (method 2) suppresses the seismic excitation better (method 1 = 57.9 t, method 2 = 43.6 t). Thus, weight is also a significant parameter, as in typical civil engineering structures,
- The location of the additional mass in the middle of the structure's mesh span (at the highest point of the dome) leads to a significant increase in the maximum values of displacements and accelerations in the case of method 1, compared to the dome without additional mass,
- The method of shaping the structure of the domes and the place of suspension of the additional mass have an impact on the response under the given excitation, because the response of the dome can be different for additional masses under the same excitation. In model II^2 (additional mass was located centrally) under the El Centro excitation, higher displacement values were obtained than in model III^2 (additional mass was located laterally), while in method 1 (model II^1 and III^1), the opposite response was noted (the largest displacements were in model III^1),
- The use of low-intensity and short-duration seismic records does not show a significant impact of suspending additional mass to the steel structure of the geodesic dome. Therefore, this effect of low-intensity and short-duration seismic records can be neglected,
- The highest values of displacements and accelerations were recorded in the horizontal direction (Y) for the strongest excitations. For weaker excitations, maximum values were also observed in the vertical direction (Z). Moreover, the direction of the maximum values is influenced by the additional mass suspended in the steel structure of the geodesic dome. Thus, it can be concluded that horizontal displacements were more dangerous for the behavior of the steel geodesic dome structure.

After the analysis, it can be concluded that further research on this topic is necessary, particularly focusing on the dynamic response of structures with various localized masses. The studies so far show that the impact is not uniform or linear, underscoring the importance of this type of research. In the future, the topic of suspended additional masses influencing the behavior of

geodesic domes is planned to continue. The aspect of analyzing these structures in response to harmonic excitation at a known time and frequency to determine dynamic characteristics is interesting.

Acknowledgments

The article was developed as part of research financed by a grant from the Rector of the Opole University of Technology, DELTA, no. TETA 262/24.

REFERENCES

1. Acito M., Mastrangelo R., Magrinelli E., Simoncelli M. Design strategies of vibration mitigation systems for an existing suspended footbridge. Eng. Struct. 2021; 249: 113279, https://doi.org/10.1016/j.engstruct.2021.113279
2. ASCE 7. Minimum Design Loads and Associated Criteria for Buildings and Other Structures (ASCE/SEI 7-22). American Society of Civil Engineers. 2022, Reston.
3. Augustyn J., Śledziewski E. Awarie konstrukcji stalowych. Arkady. 1976, Warszawa.
4. Biegus A., Rykaluk K. Collapse of Katowice fair building. Eng. Fail. Anal. 2009; 16(5): 1643–1654, https://doi.org/10.1016/j.engfailanal.2008.11.008
5. Bysiec D., Maleska, T. Numerical analysis of steel geodesic dome under seismic excitations. Materials 2021; 14(16): 4493: 1–12, https://doi.org/10.3390/ma14164493
6. Bysiec D., Maleska T. Influence of the mesh structure of geodesic domes on their seismic response in applied directions. Arch. Civ. Eng. 2023; LXIX(3): 65–78, https://doi.org/10.24425/ace.2023.146067
7. Bysiec D. Sustainable Shaping of Lightweight Structures Created According to Different Methods. Sustainability 2023; 15,3236, https://doi.org/10.3390/su15043236
8. Bysiec D., Maleska T., Janda A. Dynamic characteristic of geodesic domes with different location of mass. Life-Cycle of Structures and Infrastructure Systems. 2023; https://doi.org/10.1201/9781003323020-112
9. Bysiec D., Jaszczyński S., Maleska T. Analysis of lightweight structure mesh topology of geodesic domes. Appl. Sci. 2024; 14: 132, https://doi.org/10.3390/app14010132
10. Caglayan O., Yuksel E. Experimental and finite element investigations on the collapse of a Mero space truss roof structure—A case study. Eng. Fail. Anal. 2008; 15(5): 458–470, https://doi.org/10.1016/j.engfailanal.2007.05.005
11. Canadian Highway bridge design Code, S6–19. CSA. Canadian Standards Association. 2019, Ontario.
12. Dems K., Mroz Z. Damage identification using modal, static and thermographic analysis with additional control parameters. Comput. Struct. 2010; 88: 1254–1264, https://www.sciencedirect.com/science/article/pii/S0045794910001616
13. Eurocode 3. Design of steel structures. European Committee for Standardization. 2005, Brussels.
14. Eurocode 8. Actions Design of structures for earthquake resistance. European Committee for Standardization. 2005, Brussels.
15. Fan F., Zhi X., Li W. Analysis of the acceleration response spectra of single-layer spherical reticulated shell structures. Appl. Sci. 2022; 12(4): 2116, https://doi.org/10.3390/app12042116
16. Fanning P.J., Carden E.P. Experimentally validated added mass identification algorithm based on frequency response functions. J. Eng. Mech. 2004; 130(9): 1045–1051, https://doi.org/10.1061/(ASCE)0733-9399(2004)130:9(1045)
17. Fuliński J. Geometria kratownic powierzchniowych. The work of Wrocław Scientific Society. 1973, Wroclaw.
18. Gholizadeh S., Barati H. Topology optimization of nonlinear single layer domes by a new metaheuristic. Steel Compos. Struct. 2014; 16(6): 681–701, http://dx.doi.org/10.12989/scs.2014.16.6.681
19. Grzywiński M., Dede T., Özdemír Y. Optimization of the braced dome structures by using Jaya algorithm with frequency constraints. Steel Compos. Struct. 2019; 30(1): 47–55, https://doi.org/10.12989/scs.2019.30.1.047
20. Kaveh A., Talatahari S. Geometry and topology optimization of geodesic domes using charged system search. Struct. Multidisc. Optim. 2011; 43: 215–229, https://doi.org/10.1007/s00158-010-0566-y
21. Lapina A.P., Akay O.M., Danilova-Volkovskaya G.M., Ponomarenko A.V., Shentsova K.V. Analysis of the accidents causes at different stages of the construction object life cycle. Conf. Ser.: Mater. Sci. Eng. 2019; 698: 033011, https://doi.org/10.1088/1757-899X/698/3/033011
22. Li J., Xu J. Dynamic stability and failure probability analysis of dome structures under stochastic seismic excitation. Int. J. Struct. Stab. Dyn. 2014: 1–14, https://doi.org/10.1142/S021945541440001X
23. Maleska T., Beben D., Behaviour of soil-steel composite bridges under strong seismic excitation with various boundary conditions. Materials 2023a, 16(2): 650, https://doi.org/10.3390/ma16020650
24. Maleska T., Beben D. Effect of the soil cover depth on the seismic response in a large-span thin-walled corrugated steel plate bridge. Soil Dyn. Earthq. Eng. 2023b; 166: 107744, https://doi.org/10.1016/j.soildyn.2022.107744

25. Nair D., Ichihashi K., Terazawa Y., Sitler B., Takeuchi T. Higher mode effects of multistorey substructures on the seismic response of double-layered steel gridshell domes. Eng. Struct. 2021 ; 243, 112677, https://doi.org/10.1016/j.engstruct.2021.112677
26. Nakazawa S., Kato S., Takeuchi T., Xue S.D., Lazaro D. State of the art of seismic response evaluation methods for metal roof spatial structures. J. Int. Assoc. Shell Spat. Struct. 2012; 53: 117–130.
27. Nalitolela N., Penny J., Friswell M. Updating model parameters by adding an imagined stiffness to the structure. Mech. Syst. Signal Process. 1993; 7: 161–172, https://doi.org/10.1006/mssp.1993.1005
28. Ostachowicz W., Krawczuk M., Cartmell M. The location of a concentrated mass on rectangular plates from measurements of natural vibrations. Comput. Struct. 2002; 80(16–17): 1419–1428, https://doi.org/10.1016/S0045-7949(02)00084-6
29. Pilarska D. Two subdivision methods based on the regular octahedron for single-and double-layer spherical geodesic domes. Int. J. Space. Struct. 2020; 35(4): 160–173, https://doi.org/10.1177/0956059920956944
30. Piatkowski G., Waszczyszyn Z. Identification problems of recurrent cascade neural network application in predicting an additional mass location. Comput. Assist. Methods Eng. Sci. 2011; 3: 217–228, https://cames.ippt.pan.pl/index.php/cames/article/view/116
31. Pilarska D. Optimization approach for dome structures. The XXVII conference of Lightweight Structures in Civil Engineering, 2021; Lodz.
32. Rajendran P., Srinivasan S.M. Identification of added mass in the composite plate structure based on wavelet packet transform. Strain 2016; 52: 14–25, https://doi.org/10.1111/str.12154
33. Schling E., Wang H., Hoyer S., Pottmann H. Designing asymptotic geodesic hybrid gridshells. Comput. Aided. Des. 2022; 152: 1–17, https://doi.org/10.1016/j.cad.2022.103378
34. Shu Z., Li S., Zhang J., He M. Optimum seismic design of a power plant building with pendulum tuned mass damper system by its heavy suspended buckets. Eng. Struct. 2017; 136: 114–132, https://doi.org/10.1016/j.engstruct.2017.01.010
35. Takeuchi T., Ogawa T., Kumagai T. Seismic response evaluation of lattice shell roofs using amplification factors. J. Int. Assoc. Shell Spat. Struct. 2007; 48: 197–210.
36. Tian L., Wei J., Bai R., Zhang X. Dynamic Behavior of Progressive Collapse of Long-Span Single-Layer Spatial Grid Structures. J. Perform. Constr. Facil. 2021; 35(2), https://doi.org/10.1061/(ASCE)CF.1943-5509.0001566
37. Zhang Q., Huang W., Xu Y., Cai J., Wang F., Feng J. Analysis of key elements of single-layer dome structures against progressive collapse. Steel Compos. Struct. 2022; 42(2): 257-264, https://doi.org/10.12989/scs.2022.42.2.257
38. Zhang L., Chen Q., Zhang R., Lei T. Vibration control of beams under moving loads using tuned mass inerter systems. Eng. Struct. 2023; 275,115265, https://doi.org/10.1016/j.engstruct.2022.115265